

## Analytical investigation of biodiesel production from used frying oil using an Artificial Neural Network technique

Preeti<sup>1</sup>, Vivek Goel<sup>2\*</sup>, Sunil Kumar<sup>3</sup>,

<sup>1,2,3</sup> Gurukula Kangri (Deemed to be University) Faculty of Engineering and Technology Haridwar, Uttarakhand INDIA

\*Corresponding Author: E-mail: [vivek.goel@gkv.ac.in](mailto:vivek.goel@gkv.ac.in)

### Abstract

Used frying oil is one of the most promising feedstocks for this purpose. Therefore, the objective of this study was to synthesize biodiesel via transesterification using methanol, a potassium hydroxide (KOH) catalyst, varied reaction times, and microwave irradiation. Microwave technology was employed to enhance the efficiency of the process, potentially reducing reaction time from hours to minutes. The main aim was to examine the influence of reaction duration, catalyst concentration, and microwave power on the yield of methyl esters. An artificial neural network (ANN) was developed and trained using the Levenberg–Marquardt (LM) algorithm to model the process. Experimental results were compared with ANN predictions. The 4–45–1 topology model's  $R^2$  value of 0.9903 demonstrated the efficiency of the ANN. adj  $R^2$  value 0.9899, RMSE is 0.59 and MSE is 0.34. Range of ANN predicted value lie between 77.37 to 94.66.

Keywords :- Biodiesel, frying oil, Neural network, ANN, Production

### 1. Introduction

A sustainable and biodegradable fuel, biodiesel is composed of natural ingredients like veggies and animal lipids, residual cooking oil, and fats from animals. It is suitable for use in diesel engines with minimal to no modification when mixed with petroleum fuel to create a mixture known as biodiesel. Most people agree that fossil fuels provide the majority of the energy utilized by humanity. Due to the implementation of strict energy laws and environmental legislation, as well as the unparalleled efficiencies brought about by innovative renewable

10.48047/jocaaa.2024.33.08.226

energy technology, the world's energy demands have been expanding more slowly in recent years. Power equipment, the automotive industry, and the agricultural sector all heavily rely on diesel engines. Compared to a petrol engine, it is more durable and efficient with fuel (Mohan et al. 2014). Because of its varied chemical and physical properties and ongoing production, organic solid waste from industrial, agricultural, biomass, and municipal sources presents serious issues. To solve these problems, appropriate handling and conversion techniques are needed. Energy production and organic solid waste are linked by the chemical looping process. It seeks to accomplish sustainability using practical and profitable means. The different sources of organic solid waste and their effects on the ecosystem are highlighted in this review. It explains the use of chemical cycle conversion processes to organic solid waste, including pyrolysis, gasification, combustion, and reforming. It also provides a thorough summary of how the chemical looping process is used in the capture and use of CO<sub>2</sub> as well as the generation of bioenergy (Raja et al. 2025). Droughts and glacier melting are two major environmental problems brought on by the rise in greenhouse gases and global warming. Finding fossil fuel substitutes for internal combustion engines is therefore receiving more attention (Ibrahim 2022). Oxides of nitrogen (NO<sub>x</sub>) and carbon dioxide (CO<sub>2</sub>), two pollutants from diesel engines, are the main causes of environmental degradation, ozone layer thinning, and global warming (Elsanusi et al. 2017). Research on alternative fuels is being encouraged by the depletion of fossil fuels, environmental concerns, and strict emission regulations (Chattopadhyay and Sen 2013). Because biodiesel shares many characteristics with regular diesel, it is mostly used as a fuel substitute for diesel engines (Babu and Anand 2017). Various sources, both edible and inedible, like cottonseed, soybean, palm oil, sunflower, Karanja, and pongamia, can be used to produce it (Babu et al. 2018). Of these, used frying oil (UFO) is one of the most effective first feedstocks for the production of biodiesel since it is readily available and less expensive (Anand 2018). More emissions are produced by conventional diesel engines, exceeding

10.48047/jocaaa.2024.33.08.226

pollution standards. To further enhance engine performance and lower emissions, a contemporary system of electronic injection has been added to the diesel engine (Agarwal et al. 2015). employ the EGR technique to lower the concentration of nitrogen oxide (NO<sub>x</sub>) emissions while using an ideal DEE value of 5% in a diesel-biodiesel blend. The Ricardo WAVE program was used to do the numerical analysis. 10%, 20%, and 30% EGR amounts were employed. When 30% EGR was used, NO<sub>x</sub> emissions dropped by 59% while engine thermal efficiency only dropped by 5.6%. Furthermore, the heat release rate dropped by 27.6%, the ignition delay rose by 5.3%, and the combustion duration extended from 33.7° to 48.8° when 30% EGR was used. These findings suggest that the concentration of NO<sub>x</sub> emissions from diesel engines can be considerably reduced by using EGR and DEE (Youssef and Ibrahim 2024).

According to the optimization result, the ideal parameters were reached at 61.78 °C, a methanol to oil molar ratio of 9.25:1, and a catalyst concentration of 0.86 weight percent. 94.47% was the maximum biodiesel yield that was anticipated. For 1.5 hours, the reaction was conducted at a steady 500 rpm reaction speed. Livistona jenkinsiana oil (LJO) is the best source of biodiesel, according to the physicochemical characteristics of the final product (Ahamed et al. 2023). Efficiency was greatly increased by decreasing series resistance and raising shunt resistance; however, performance was reduced at higher temperatures. Excellent results were obtained by the cell after optimization: VOC of 1.0825 V, JSC of 31.423 mA/cm<sup>2</sup>, FF of 87.33%, and PCE of 29.74%. Additionally, it demonstrated almost 100% QE in the visible spectrum, guaranteeing robust photon absorption. These results offer a foundation for creating effective GaAs solar cells and tackling issues with material optimization and temperature control (Shah et al. 2025). Using COMSOL Multiphysics software, this study examined the noteworthy performance of thermoelectric modules (TEMs) made of bismuth telluride, copper (Cu), and aluminum oxide materials, paying special attention to examining different leg

geometries.

In this design, the thicker alumina layer provides efficient electrical insulation, while the thin copper layer maximizes heat conduction. Finally, a  $\text{Bi}_2\text{Te}_3$  TEM with ideal dimensions of  $1.00\text{ mm} \times 1.00\text{ mm} \times 2.75\text{ mm}$ , an insulator thickness of  $0.50\text{ mm}$ , and a conductor thickness of  $0.125\text{ mm}$  is advised. The particular setup demonstrates exceptional TEG functioning and creates intriguing opportunities for additional study in this area (Hasan et al. 2024b). Copper, bismuth telluride, and alumina are used in the construction of TEC. Specifically,  $\text{Bi}_2\text{Te}_3$  acts as the p- and n-type thermoelectric (TE) legs between the Cu layers, Cu operates as a conductor, and  $\text{Al}_2\text{O}_3$  acts as an electric insulator for the top and bottom layers. The study looked at the effects of varying TE leg shapes (square and rectangular) and heights ( $1.5$ ,  $2\text{ mm}$ , and  $2.5\text{ mm}$ ) on TEC performance. It examined a number of variables, including total net energy rate, normalized current density, electric potential, and temperature gradient. It is advised to employ a  $\text{Bi}_2\text{Te}_3$  TEC with ideal measurements of  $1.00\text{ mm} \times 1.00\text{ mm} \times 1.5\text{ mm}$ , a pitch of  $0.50\text{ mm}$ , and conductor and insulator thicknesses of  $0.125\text{ mm}$  and  $0.375\text{ mm}$ , respectively. The  $12\text{ mm} \times 10\text{ mm} \times 2.5\text{ mm}$  performance specifications include the following values (maximum):  $73.94\text{ K}$  temperature difference,  $2.52\text{ V}$  voltage,  $3.00\text{ A}$  current,  $4.42\text{ W}$  maximum heat load ( $\Delta T = 0$ ),  $0.84\ \Omega$  resistance, and a figure of merit of  $0.002377\text{ 1/K}$  (Hasan et al. 2024a). The possibility of using waste plastic oil (WPO) from plastic pyrolysis as a substitute fuel for diesel engines, with an emphasis on a study conducted. In contrast to diesel fuel, their study examined the emissions and composition of plastic pyrolysis oils (PPOs) derived from different polymer-based fuels. Key findings include that PP PPOs showed lower  $\text{NO}_x$  emissions whereas LDPE and HDPE PPOs showed greater CO emissions under heavy loads. Less unburned hydrocarbon was produced by lighter loads, even though the PPOs had a higher hydrocarbon concentration. When nanoscale deposits or particles are present, the Seebeck coefficient may rise, improving the overall performance of TE. This study emphasizes the material's adaptability for energy

10.48047/jocaaa.2024.33.08.226

harvesting, cooling devices, and TEGs. This work specifically examines the dynamics of the electric potential inside the TEM, demonstrating its sensitivity to temperature variations and efficiency in energy conversion. The need of controlling temperature in order to maximize TEG performance is demonstrated by the inverse relationship between electric potential and surface temperature. Normalized current density studies indicates that 3.5628 V is the ideal electric potential for boosting TEG efficiency (Hasan et al. 2024c). They used SCAPS-1D simulations to optimize a CIGS-based (Al/ZnO/ZnMnO/CIGS/Cu<sub>2</sub>O/Ni) thin-film solar cell, attaining notable efficiency gains through accurate parameter modifications. With acceptor and donor concentrations of  $10^{17} \text{ cm}^{-3}$  and  $10^{16} \text{ cm}^{-3}$ , respectively, the optimal design includes a 3000 nm CIGS absorber layer, a 50 nm ZnO window layer, a 50 nm ZnMnO buffer layer, and a 10 nm Cu<sub>2</sub>O ER-HTL. A remarkable PCE of 31.84% was achieved with these adjustments, with  $V_{OC} = 1.0112 \text{ V}$ ,  $J_{SC} = 38.80 \text{ mA/cm}^2$ , and  $FF = 81.13\%$ . Achieving an ideal series resistance of  $0 \Omega \text{ cm}^2$  and a shunt resistance of  $1 \times 10^6 \Omega \text{ cm}^2$  further reduced resistive losses by lowering voltage drop and current leakage. Higher temperatures have a detrimental effect on efficiency, mostly because they reduce  $V_{OC}$  and  $FF$ , according to temperature analysis conducted between 290 and 400 K (Sikder et al. 2025). All things considered, PPOs have the potential to lower emissions, deal with plastic waste, and offer workable diesel engine substitutes. The WPO is a workable solution because it is compatible with current engine systems, unlike some alternatives. This highlights its promise as a cleaner alternative fuel (Modi and Patel 2023). The most important factor influencing the particular fuel consumption was found to be the engine load, which was followed by the fuel type, injection pressure, and compression ratio. The suggested model successfully fits the experimental data, as evidenced by the high R-squared (99.35%) and adjusted R-squared (98.02%) data. In conclusion. The performance of the CI engine is efficiently optimized under a variety of operating circumstances using the

10.48047/jocaaa.2024.33.08.226

RSM-based model. It improves engine performance and sustainability by drastically cutting down on the time and effort needed to adjust engine design factors (Modi and Patel 2024a).

It is possible to create biodiesel via chemical, biological, supercritical, and other techniques. The primary industrial production technique used nowadays is base- or acid-catalyzed transesterification. There are social and economic advantages to biodiesel. The creation of biodiesel can help eliminate home wastes like used cooking oil and reduce pollution while offering a novel means of converting agricultural goods. It can also benefit the environment (Banković-Ilić et al. 2012; Abbaszaadeh et al. 2012; Verma and Sharma 2016). These days, there is a lot of interest in producing biodiesel in an environmentally responsible and sustainable manner. The concepts of green chemistry are utilized to carry out the chemical process in a sustainable manner, hence minimizing adverse environmental effects (Andraos and Sayed 2007). ANN techniques, which were developed based on the neuro-evolution principle, were used for modeling and prediction. Early in the 1940s, the idea of the ANN was developed. This mathematical model, which draws inspiration from the actual brain, is made up of a network of linked processing units known as neurons. The current study examines how various ethanol mixes (E0, E5, E10, and E15) with gasoline 92 affect a GX35 four-stroke engine's emissions and performance metrics at various engine speeds. According to the data, increasing the amount of ethanol causes an average increase in brake power (BP), brake thermal efficiency (BTE), and CO<sub>2</sub> emissions of 2.7%, 1%, and 1.1%, respectively, over the speed range. In the meantime, it reduces exhaust gas temperature (EGT), brake-specific fuel consumption (BSFC), HC, and CO emissions by an average of 28 °C, 3%, 15 ppm, and 0.18%, respectively. Additionally, an Artificial Neural Networks (ANN) model is developed in this study to forecast the emissions and performance of spark ignition (SI) engines (Hofny et al. 2024). The Response Surface Method, which is based on full factorial CCRD and NSGA-II, was used to conduct the tests. To optimize the combustion characteristics (brake-specific fuel consumption),

10.48047/jocaaa.2024.33.08.226

performance characteristics (brake thermal efficiency), and emission parameters (CO, NO<sub>x</sub>, HC) in NSGA II, mathematical models for BSFC (brake-specific fuel consumption), BTE (brake thermal efficiency), and emission (CO, NO<sub>x</sub>, and unburned HC) have been proposed using regression equations. Since the goal of this inquiry is to optimize BTE and minimize BSFC, CO, NO<sub>x</sub>, and HC, a multiobjective optimization problem has been established (Kumar et al. 2023). ANNs may estimate behavior when there is incomplete data available and can simulate non-formal class distribution. ANNs also have the following benefits: i) sample sets can be used to construct them; ii) It is not required to understand the processes' phenomenology; iii) An ANN model can provide excellent predictions for fresh input datasets after it is established.; iv) Several input-output relationships can be modeled at the same time. Because of these characteristics, ANNs can be used for a variety of systems and issues. A yeast fermentation bioreactor's temperature is controlled and dynamic modeling is done using artificial neural networks (ANNs), which are related to biochemical processes. Key metrics from the training set for the LM10TP architecture included an exceptional R-squared value of 1, which indicated a perfect match with a mean square error (MSE) of 1.5143E-06 and a root mean square error (RMSE) of 0.0012. With an R-squared value of 0.9999, an RMSE of 0.0011, and an MSE of 1.2185E-06, the validation set also demonstrated strong performance metrics (Modi and Patel 2024b). Artificial Neural Networks have proven to be **more robust, flexible, and accurate** than traditional modelling approaches in biodiesel production. Their ability to handle complex, nonlinear datasets and their integration with optimization tools make them **highly appropriate** for both laboratory research and industrial-scale biodiesel production (Chung 2012; Wiloso et al. 2012; Pradhan et al. 2016; Atef et al. 2018) .

An ANN is an extremely potent mathematical tool that has demonstrated its effectiveness across numerous domains. In petroleum science, artificial neural networks have been utilized to simplify complex computations. The ANN model is mostly used to forecast the yield of

10.48047/jocaaa.2024.33.08.226

biodiesel from various feedstocks. For an ANN to learn anything about the problem, it needs examples of solutions. When fresh data are received, the machine can forecast outcomes after learning. A computational method called artificial neural networks (ANNs) aims to replicate the brain's neurological processing capacity. With a 4–45–1 topology, the ANN model's  $R^2$  score of 0.9903 demonstrated the efficiency of the network architecture. The outcomes showed that the target values provided fit the ANN model quite well. In this context, **Artificial Neural Networks (ANNs)** offer a powerful data-driven approach capable of modelling complex systems without requiring explicit assumptions about underlying mechanisms. ANNs can learn from historical data to predict biodiesel yield with high accuracy, optimize process conditions, and identify critical control parameters. By leveraging ANN models, researchers and industry practitioners can achieve more reliable process control, reduce experimental costs, and accelerate the development of more efficient biodiesel production systems.

This study explores the application of ANN in modeling and predicting biodiesel yield, aiming to demonstrate its potential as a robust alternative to conventional modeling approaches in the field of biofuel research.

The first section of this study presents the experimental results of biodiesel yield produced from spent frying oil. The tests used frying oil methyl ester as biodiesel and methanol as alcohol. The Levenberg-Marquardt (LM) algorithm approach was then used to make predictions using experimental data.

## 2. Materials and Method

Comparable to traditional or fossil diesel, biodiesel is an alternate fuel. Utilizing vegetable oil alone, animal fats or oil, and leftover cooking oil, biodiesel can be made. It is a procedure known as transesterification. To create the mixture, potassium hydroxide (KOH, 99.0% extra pure, in pellet form) and methanol (99% special grade). A Box-Behnken design (BBD) was used for experimental series. The range of four variables needed for a process called

10.48047/jocaaa.2024.33.08.226

transesterification is Time (5-7 minutes), Catalyst (0.5 – 1.5 grams), Methanol/Oil (30-50 %), and Power of microwave (200-300 Watts) respectively. the parameters and their levels were chosen based on pilot experimental work done on the developed set up (Khedri et al. 2019; Kumar 2021).

### 3. Biodiesel Generation

The Figure-1 represents a Microwave-Assisted Apparatus, a setup commonly used for Biodiesel Production. Here is an explanation of each labelled component: **Condenser:** This cools the vapor produced, turning it back into liquid form. It's usually water-cooled and placed vertically to allow condensed liquid to flow down. **DC Motor:** The motor powers the stirrer, which helps ensure uniform. **Domestic Microwave:** Acts as the heat source. Microwaves rapidly heat the solution inside the flask, which accelerates the distillation process compared to conventional heating methods. This apparatus combines the benefits of microwave heating (fast, energy-efficient). In the process of producing biodiesel, a reaction known as transesterification. This process chemically transforms various oils; when methanol and triglycerides combine to form glycerine and esters. A catalyst is essential to facilitate this reaction, which occurs in three consecutive reversible steps. Initially, triglycerides convert to diglycerides, followed by conversion to monoglycerides. Finally, esters and glycerine are obtained in the last step of the process.

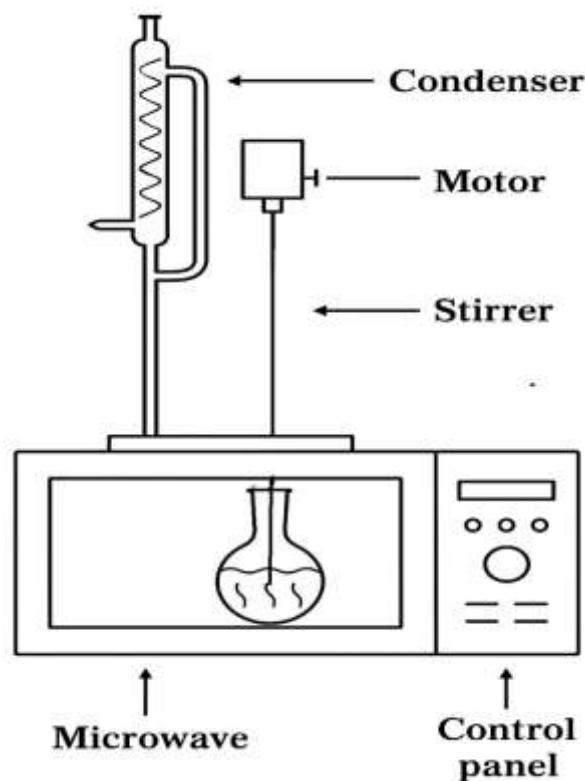


Figure-1 Experimental Setup

#### 4. Artificial Neural Network

Artificial neural networks (ANN) are a potent class of mathematical modelling tools. For ANN to build the necessary model, a great deal more testing would be needed. On the other hand, if there was statistical significance in the data in both the output and input domains, ANN could function well even with relatively little data. Which applies to experiment design. It consists of fundamental neural units, which are computational units coupled in a parallel configuration. These portions resemble the physiological neurons found in the brain of an individual. To forecast the process under consideration, a neuro-evolutive technique was utilized (The yield response is calculated about the temperature, molar ratio, catalyst concentration, and reaction time.).

A three-layered feed-forward neural network was used in this investigation. Where the output layer was a purelin, the hidden layer was a tansig, and the input layer was a tansig. Among all

10.48047/jocaaa.2024.33.08.226

the backpropagation (BP) methods, the Levenberg-Marquardt learning strategy was selected due to its efficiency and effectiveness (Banza and Rutto 2023). *trainlm* method was chosen because of its low computational time and application. This method outperforms its competitors by updating weights following Levenberg-Marquardt optimisation (Arunyanart et al. 2024). The hidden layer with 45 neurons, the output layer, and the input layer make up the ANN architecture. Figure-2 displays the ANN architect structure which is self-explanatory. The green square labeled "Input" represents the input layer, which has 4 units (indicated by the number "4"). This means the network receives input data in a 4-dimensional format (4 features). The hidden layer has 45 units (neurons), as shown by the number "45" at the bottom of the hidden layer box. The output layer has 1 unit, indicating that the network produces a single output value. It functions similarly to a "black box" model, needing neither an explicit statement of the equations in mathematics that control the system being studied nor any knowledge about the system. The goal was to increase the biodiesel yield.

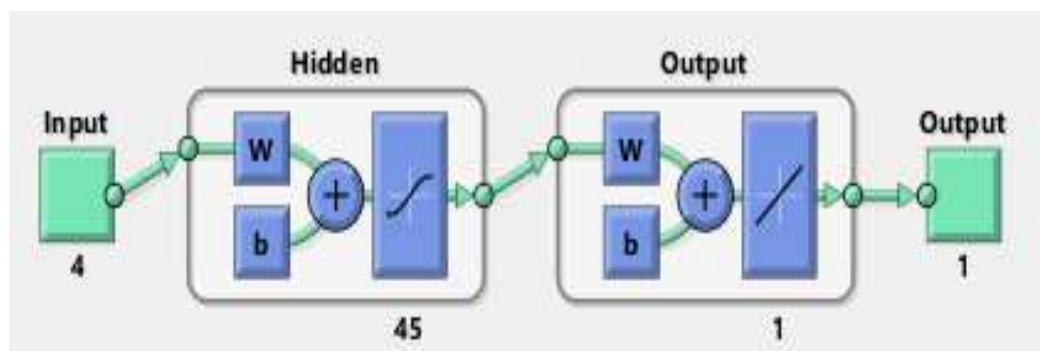


Figure 2. Diagram of Artificial neural network

## 5. Results and discussions

According to specified parameters, the biodiesel yield values of the blended utilized frying oil were assessed. The Figure Horizontal axis shows the deviation of the factors from a reference or baseline point, presented in coded units. Vertical axis (YIELD %) The response variable, yield percentage, is on the Y-axis, ranging from about 75% to 100%. Factors (A, B, C, D): Each

10.48047/jocaaa.2024.33.08.226

curve represents a different factor affecting the yield. Catalyst (Factor B) shows a strong influence on the yield, as it has a noticeable curve and declines as the deviation increases. This indicates that changes in Factor B have a significant effect on yield. Other factors show flatter curves, indicating that changes in these factors have a smaller impact on yield within the range tested. The plot suggests that Catalyst is the most critical factor to control for optimizing yield, while the other factors have a relatively negligible effect on yield in the studied range. Choosing the right number of neurons in the hidden layer of a neural network is a crucial decision that involves balancing model capacity and the risk of overfitting. While adding more neurons can indeed increase the likelihood of overfitting, there are several situations where using a higher number of neurons in the hidden layer can be beneficial. Choosing the number of neurons is often done through the trial and error method displayed in Table 1. Techniques like cross-validation can help assess the model's performance with different numbers of neurons and identify the optimal balance. From Table 45 neurons give better results as compared to another topology. The ANN prediction model development process involves multiple steps, as seen in Figure 4. Data was first gathered via several experiments. The selection of the training method and step, wherein an input is fed and taught to create the intended output, is a crucial aspect of ANNs. When an error occurs, that is, when the disparity between the intended.

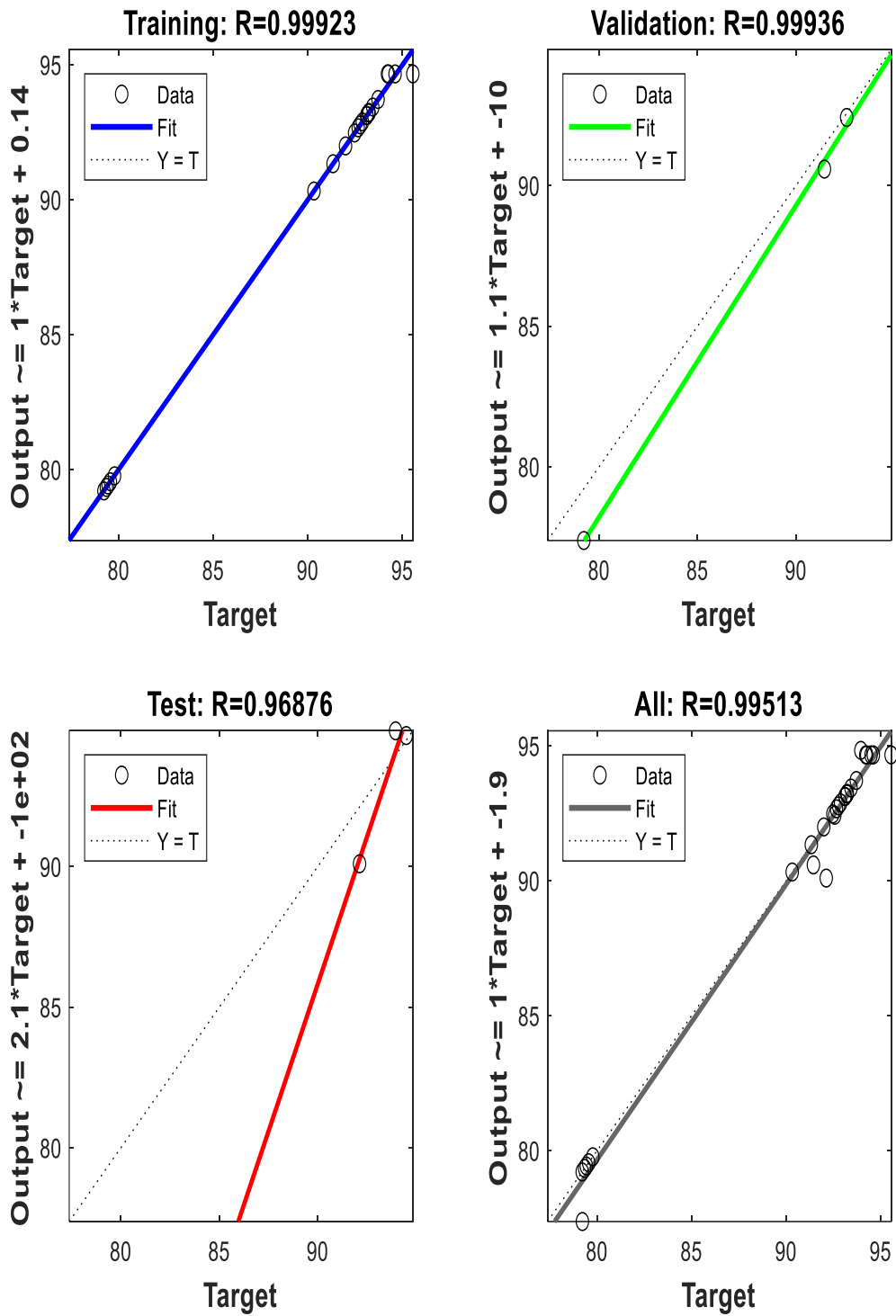


Figure 3. Validation, Training, Testing, and Overall scatter diagram.

**Table 1.** Statistical value for the yield of biodiesel using ANN.

Algorithm	Topology	Training	Validation	Testing	Overall	R <sup>2</sup>	Regression line
Levenberg Marquardt	4-5-1	0.99458	0.98783	0.99719	0.99307	0.9862	Y=1.002X-0.0657
	4-10-1	0.99926	0.96438	0.99813	0.99323	0.9865	Y=1.0214X-1.216
	4-15-1	0.98506	0.91227	0.99001	0.96765	0.9363	Y=1.051X-5.15
	4-20-1	0.98503	0.99493	0.9577	0.97077	0.9424	Y=1.021X-1.363
	4-25-1	0.99914	0.99327	0.99149	0.95913	0.9199	Y=0.979X+1.556
	4-30-1	0.98129	0.90789	0.95643	0.90934	0.8269	Y=1.073X-6.052
	4-35-1	0.99955	0.96202	0.097076	0.88014	0.7746	Y=0.9711X+2.461
	4-40-1	0.99997	0.95464	0.94908	0.92647	0.8583	Y=1.076X-6.387
	<b>4-45-1</b>	<b>0.99923</b>	<b>0.99936</b>	<b>0.96876</b>	<b>0.99513</b>	<b>0.9903</b>	<b>Y=1.02X-1.903</b>
	4-50-1	0.99174	0.99923	0.94601	0.63793	0.4070	Y=0.8294X+14.59
	4-55-1	0.97513	0.98457	0.98382	0.75547	0.5707	Y=1.18X-9.19
	4-60-1	0.99933	0.98511	0.98348	0.91582	0.8387	Y=0.9345X+5.184
	4-65-1	0.99922	0.99793	0.98612	0.22418	0.0503	Y=0.4341X+47.38
	4-70-1	0.98943	0.95448	0.97516	0.84687	0.7172	Y=1.021X-1.107
	4-75-1	0.99886	0.95505	0.90305	0.82042	0.6731	Y=1.835X-79.16
	4-80-1	0.99933	0.91481	0.99003	0.77329	0.5980	Y=1.184X-17.21
	4-85-1	0.99906	0.99758	0.93446	0.8487	0.7203	Y=1.12X-11.03
	4-90-1	0.99996	0.95122	0.90085	0.82776	0.6852	Y=1.234X-22.12
	4-95-1	0.99922	0.9709	0.95865	0.77335	0.5981	Y=0.9465X+3.275
	4-100-1	0.99933	0.90797	0.97632	0.28401	0.0807	Y=0.7592X+19.26

The expression for R square is

$$R^2 = 1 - \sum_{i=1}^n \frac{(y_i - y_{di})^2}{(y_{di} - y_m)^2}$$

The Regression formula is

$$Y = mx + c$$

where  $m$  is the slope,  $y$  is the predicted score, of the line, and  $c$  is the  $y$ -intercept.

where  $y_m$  is the average of the real values,  $y_{di}$  Is the actual value, and  $y_i$  Is the forecast value using the neural network model. The number of points is represented by  $n$ .

Table 1 makes it evident that, when compared to other algorithms, the Levenberg–Marquardt method with topology 4–45–1 produces the optimal outcomes.

**Table 2.** Predicted and Experimental feedback of variables.

S.no.	A-Time (minute)	B-Catalyst (wt.%)	C-Methanol/Oil (%)	D- Power	Yield(%) (Experime ntal)	ANN Prediction (%)
1	0	0	0	0	90.32	90.31
2	0	+1	0	-1	79.43	79.43
3	0	0	+1	+1	94.21	94.66
4	0	0	+1	-1	92.12	90.09
5	0	+1	+1	0	79.77	79.77
6	0	-1	+1	0	95.55	94.66
7	-1	0	-1	0	79.34	79.34
8	+1	0	-1	0	91.99	91.99
9	0	+1	0	+1	93.22	93.22

10.48047/jocaaa.2024.33.08.226

10	+1	0	0	-1	92.77	92.77
11	0	-1	-1	0	79.55	79.55
12	0	0	0	0	91.33	91.33
13	+1	0	+1	0	94.61	94.66
14	0	0	0	0	93.95	94.83
15	0	0	-1	-1	79.22	77.37
16	0	0	-1	+1	92.88	92.88
17	-1	0	+1	0	92.57	92.42
18	0	-1	0	+1	94.26	94.66
19	0	0	0	0	93.23	93.22
20	0	-1	0	-1	93.43	93.43
21	-1	0	0	+1	93.11	93.11
22	-1	+1	0	0	91.44	90.58
23	+1	0	0	+1	93.71	93.71
24	0	+1	-1	0	94.49	94.66
25	+1	+1	0	0	92.66	92.66
26	0	0	0	0	79.21	79.21
27	+1	-1	0	0	93.12	93.12
28	-1	0	0	-1	92.47	92.47
29	-1	-1	0	0	93.21	93.21

Table-3 ANN output details

S.NO	Technique	R <sup>2</sup>	ADJ-R <sup>2</sup>	RMSE	MSE	SSE
1	ANN	0.9903	0.9899	0.59	0.348	9.4

**Table 4** Comparison of biodiesel production with previous studies

S.NO	Feedstock	Model	Model Performance (R <sup>2</sup> )	Refs
1	Palm Kernel Oil	ANN & ANFIS	0.996 & 0.994	(Betiku et al. 2016)
2	WCO	ANN	0.999	(Buasri et al. 2023)
3	Crude oil	ANN	0.977	(Hashemi Fath et al. 2018)
4	Vegetable Oils	ANN & ANN-PSO	0.993 & 0.972	(Arunyanart et al. 2024)
5	Animal Fa	ANN & ANFIS	0.989 & 0.993	(Mwenge and Rutto 2025)
76	Used Frying Oil	ANN	0.9903	This Work

The real experimental values were contrasted with the anticipated replies that the ANN produced. By analyzing the R<sup>2</sup> values, the models' accuracy created using ANN was assessed. Finding the equation of a line that fits the data is our goal during analysis. The best match is shown in Figure -3 as a solid line. Figure-4 describe This is a flowchart representing the workflow of a ANN model development process, specifically focusing on using Mean Square Error (MSE) as the performance metric. **Collection of Data** : Gather the dataset that will be used to train and evaluate the model. **Selection of Algorithm**: Choose an appropriate machine learning algorithm. **Set Learning Parameters**: Configure hyperparameters like number of epochs, Neuron etc., before training begins. **Training**: Feed the training data into the selected algorithm to build the model. **Find Mean Square Error (MSE)**: After training, the MSE is calculated to assess how well the model is performing. Lower MSE indicates better model

10.48047/jocaaa.2024.33.08.226

accuracy. **Decision:** This decision diamond checks whether the calculated MSE meets a predefined threshold or acceptable level. **If YES:** The model is considered sufficiently accurate, and the Result is accepted. **If NO:** Go back to adjust the **learning parameters**, and retrain the model until an acceptable MSE is achieved. Fig-4 to shows how the response is influenced by small changes in the input variables around a reference point. **Y-axis (Yield):** Yield in percentage (%). **X-axis shows** Deviation from a reference point in coded units (usually scaled from -1 to 1). **Lines A (Time), B (Catalyst), C (Methanol/oil) & D (Power):** These represent the different input variables (factors) being perturbed one at a time while the others are held constant. **Black dot:** The reference point where all variables are at their centre or baseline values. The steeper the curve, the more sensitive the response (Yield) is to that variable. **Variable B** has the most pronounced effect on Yield—it shows a steep downward trend as deviation increases positively, indicating that increasing this variable too much can significantly decrease the yield. **Variables A, C, and D** have relatively flatter curves, suggesting they have a smaller impact on Yield within the tested range. All points should sit on the line of unit slope (also known as the best-fit line) if the agreement is perfect. For this ANN model, the maximum values of R-square, overall R, and topology were 0.9903, 0.99923, and 4-45-1, respectively. Figure 3 displays the obtained scatter plots for training, test, validation, and total ANN data. ANN output details are given in table-3, Which depict the results of ANN are acceptable. **R<sup>2</sup>** (R-squared = 0.9903): Indicates the proportion of variance in the variables that is predictable from the Actual variable. Value close to 1.0 means a very strong fit of the variance. **Adjusted R<sup>2</sup>** (Adj-R<sup>2</sup> = 0.9899): Slightly lower than R<sup>2</sup>; this prevents overfitting by penalizing unnecessary predictors. Still very close to 1, indicating a well-generalized model. **RMSE** (Root Mean Squared Error = 0.59): Lower RMSE means better predictive accuracy. Here, the error is small, so predictions are highly accurate. **MSE** (Mean Squared Error = 0.348): Also low, consistent with the low RMSE. **SSE** (Sum of Squared Errors = 9.4): Again, a **low**

10.48047/jocaaa.2024.33.08.226

**value** suggests the model's predictions are close to the actual values. Figure-6 depicts the curve fitting of Actual and predicted values. The regression curve follows a linear trend, suggesting a strong positive correlation between Actual and Predicted Value. The data points are closely clustered around the regression line, which indicates: **High accuracy** of the model. **Low variance** or error. **high  $R^2 = 0.9903$** . Table 4 compares results obtained in this study with previous studies, highlighting the best fit to be the one with  $R^2$  close to 1.

## 6. Limitations

The ANN models are trained on specific datasets generated under controlled experimental conditions. The accuracy of these models may decrease when applied to different feedstocks, catalysts, or operating conditions not represented in the training data. Addressing this limitation would require additional training datasets encompassing diverse feedstocks and reaction conditions. Future research could focus on different catalyst and ultrasonic heating set up. Advanced techniques, such as Shapley Additive Explanations, Fuzzy and Machine Learning could be explored to enhance model interpretability. While the environmental benefits of the proposed approach are evident, a comprehensive economic analysis, would be necessary to evaluate its feasibility on an industrial commercial scale.

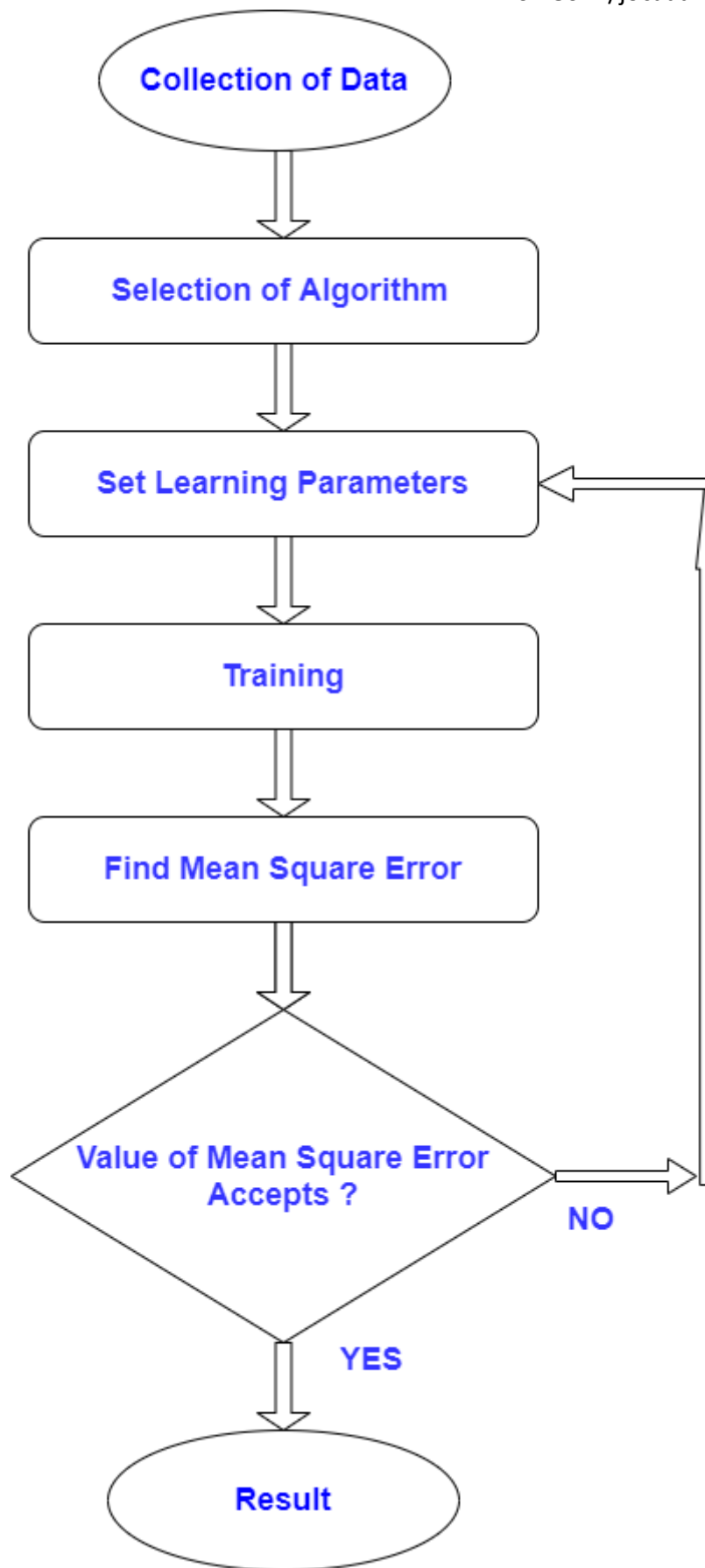


Figure 4. Diagram for ANN Working

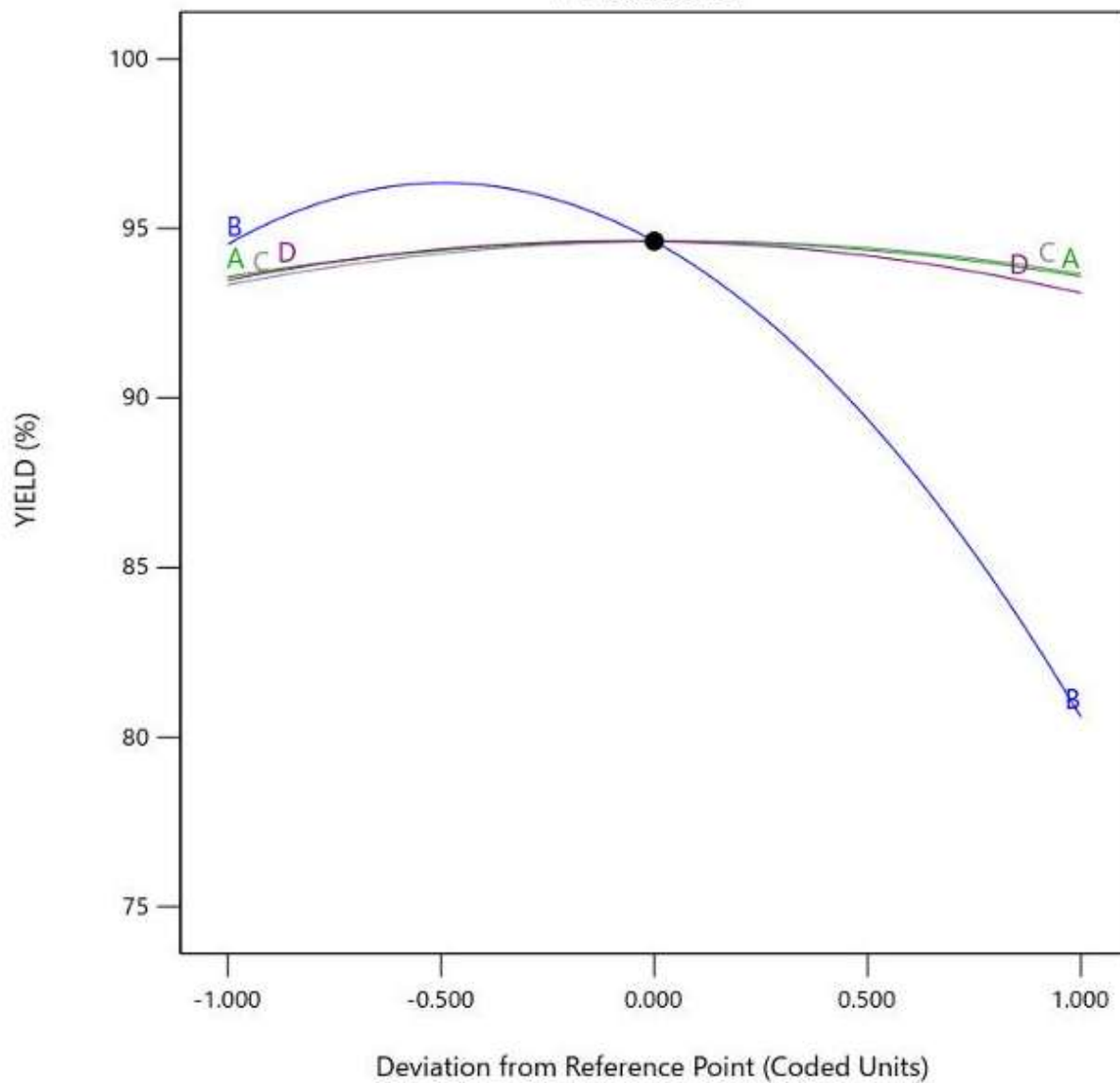


Figure- 5 Parametric effect of yield

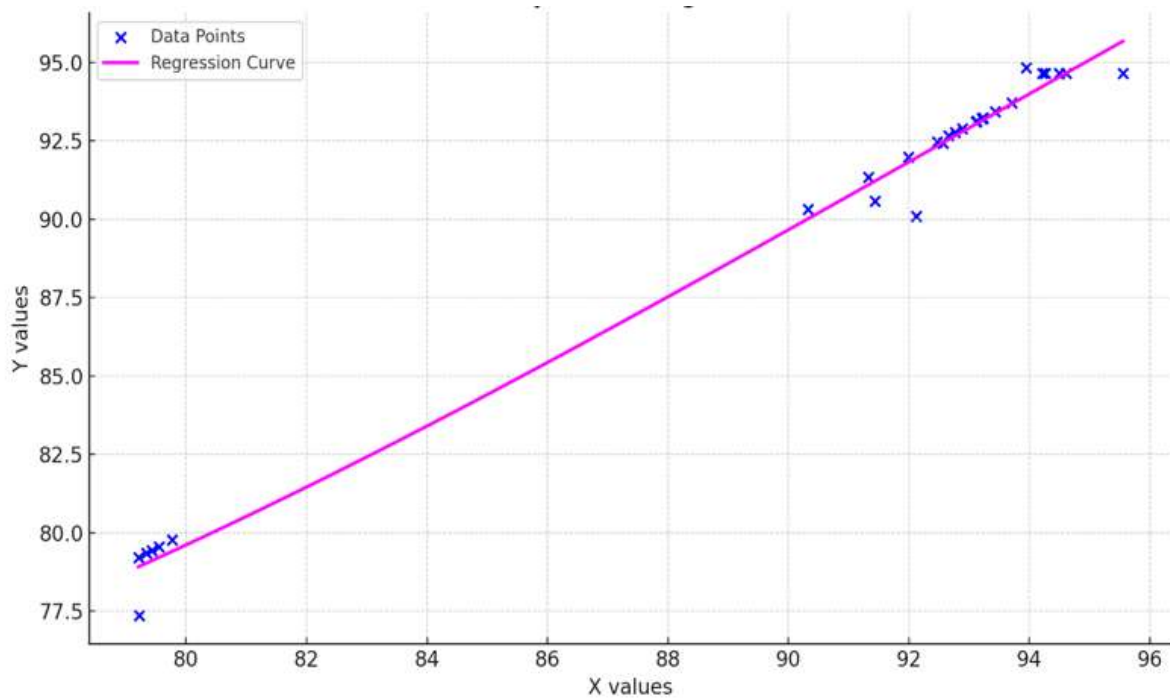


Figure-6 Curve between Actual and Predicted Value

## Conclusion

This study investigated the influence of various process parameters on the yield of biodiesel produced from a combination of used frying oils. Key variable— catalyst concentration, was found to significantly affect the blend yield. Biodiesel, a viable alternative to conventional fossil diesel, can be derived from vegetable oils, animal fats, and Used frying oils through a process known as transesterification. For this process, potassium hydroxide (KOH, 99.0% purity) and methanol (special grade, 99%) were employed as the catalyst and alcohol, respectively. The transesterification reaction was the primary method used for biodiesel synthesis with microwave heating set up. An artificial neural network (ANN) approach was applied to predict biodiesel yield. The model utilized a 4–45–1 topology, achieving a high  $R^2$  value of 0.9903, indicating the ANN's strong predictive performance. The metrics further highlighted ANN accuracy, with values of adj 0.9899 ( $R^2$ ) 0.34 (MSE), 0.59(RMSE) and 9.4

(SSE). ANNs are powerful tools for mathematical modelling, and the results demonstrated an excellent fit between predicted and actual yield values. The minimal deviation between these values confirms the ANN model's accuracy in forecasting biodiesel yield. Overall, the findings highlight the potential of artificial neural networks as effective tools for both modelling and optimizing biodiesel production processes.

**Author contributions**

Sunil Kumar – editing, re writing, concept  
Preeti- Writing, Drafting, Experimentation  
Vivek Goel- supervising

**Funding** No external funding is required.

**Data availability**

All the data analyzed are included in this paper.

**Declarations****Conflict of interests**

The authors declare no competing interests.

**Consent for publication**

All authors consent to the publication of this paper.

**Ethics approval** This is not applicable.

**Consent to participate** This is not applicable.

**Competing interests** The authors declare no competing interests.

**References**

- Abbaszaadeh A, Ghobadian B, Omidkhah MR, Najafi G (2012) Current biodiesel production technologies: A comparative review. *Energy Conversion and Management* 63:138–148. <https://doi.org/10.1016/j.enconman.2012.02.027>
- Agarwal AK, Dhar A, Gupta JG, Woong Il Kim, Choi K, Lee CS, Park S (2015) Effect of fuel injection pressure and injection timing of Karanja biodiesel blends on fuel spray, engine performance, emissions and combustion characteristics. *Energy Conversion and Management* 91:302–314. <https://doi.org/10.1016/j.enconman.2014.12.004>
- Ahamed MS, Lingfa P, Chandrasekaran M (2023) RSM modelling and optimization for performance evaluation of biodiesel production process from *livistona jenkinsiana* using NaOH as a catalyst. *Eng Res Express* 5:045043. <https://doi.org/10.1088/2631-8695/ad069b>

10.48047/jocaaa.2024.33.08.226

- Anand R (2018) Simultaneous Control of Oxides of Nitrogen and Soot in CRDI Diesel Engine Using Split Injection and Cool EGR Fueled with Waste Frying Oil Biodiesel and Its Blends. In: Sharma N, Agarwal AK, Eastwood P, et al. (eds) Air Pollution and Control. Springer, Singapore, pp 11–44
- Andraos J, Sayed M (2007) On the Use of “Green” Metrics in the Undergraduate Organic Chemistry Lecture and Lab To Assess the Mass Efficiency of Organic Reactions. *J Chem Educ* 84:1004. <https://doi.org/10.1021/ed084p1004>
- Arunyanart P, Simasatitkul L, Juyploy P, Kotluklan P, Chanbumrung J, Seeyangnok J (2024) The prediction of biodiesel production yield from transesterification of vegetable oils with machine learning. *Results in Engineering* 24:103236. <https://doi.org/10.1016/j.rineng.2024.103236>
- Atef N, Badra J, Jaasim M, Im HG, Sarathy SM (2018) Numerical investigation of injector geometry effects on fuel stratification in a GCI engine. *Fuel* 214:580–589. <https://doi.org/10.1016/j.fuel.2017.11.036>
- Babu D, Anand R (2017) Effect of biodiesel-diesel-*n*-pentanol and biodiesel-diesel-*n*-hexanol blends on diesel engine emission and combustion characteristics. *Energy* 133:761–776. <https://doi.org/10.1016/j.energy.2017.05.103>
- Babu D, Karvembu R, Anand R (2018) Impact of split injection strategy on combustion, performance and emissions characteristics of biodiesel fuelled common rail direct injection assisted diesel engine. *Energy* 165:577–592. <https://doi.org/10.1016/j.energy.2018.09.193>
- Banković-Ilić IB, Stamenković OS, Veljković VB (2012) Biodiesel production from non-edible plant oils. *Renewable and Sustainable Energy Reviews* 16:3621–3647. <https://doi.org/10.1016/j.rser.2012.03.002>
- Banza M, Rutto H (2023) Modelling of adsorption of nickel (II) by blend hydrogels (cellulose nanocrystals and corn starch) from aqueous solution using adaptive neuro-fuzzy inference systems (ANFIS) and artificial neural networks (ANN). *The Canadian Journal of Chemical Engineering* 101:1906–1918. <https://doi.org/10.1002/cjce.24603>
- Betiku E, Odude VO, Ishola NB, Bamimore A, Osunleke AS, Okeleye AA (2016) Predictive capability evaluation of RSM, ANFIS and ANN: A case of reduction of high free fatty acid of palm kernel oil via esterification process. *Energy Conversion and Management* 124:219–230. <https://doi.org/10.1016/j.enconman.2016.07.030>
- Buasri A, Sirikoom P, Pattane S, Buachum O, Loryuenyong V (2023) Process Optimization of Biodiesel from Used Cooking Oil in a Microwave Reactor: A Case of Machine Learning and Box–Behnken Design. *ChemEngineering* 7:65. <https://doi.org/10.3390/chemengineering7040065>
- Chattopadhyay S, Sen R (2013) Fuel properties, engine performance and environmental benefits of biodiesel produced by a green process. *Applied Energy* 105:319–326. <https://doi.org/10.1016/j.apenergy.2013.01.003>

10.48047/jocaaa.2024.33.08.226

- Chung W (2012) Using the fuzzy linear regression method to benchmark the energy efficiency of commercial buildings. *Applied Energy* 95:45–49. <https://doi.org/10.1016/j.apenergy.2012.01.061>
- Elsanusi OA, Roy MM, Sidhu MS (2017) Experimental Investigation on a Diesel Engine Fueled by Diesel-Biodiesel Blends and their Emulsions at Various Engine Operating Conditions. *Applied Energy* 203:582–593. <https://doi.org/10.1016/j.apenergy.2017.06.052>
- Hasan MdK, Haque MdM, Üstüner MA, Mamur H, Bhuiyan MRA (2024a) Optimizing the performance of Bi<sub>2</sub>Te<sub>3</sub> TECs through numerical simulations using COMSOL multiphysics. *Journal of Alloys and Metallurgical Systems* 5:100056. <https://doi.org/10.1016/j.jalmes.2024.100056>
- Hasan MK, Üstüner MA, Korucu H, Mamur H, Bhuiyan MRA (2024b) Influence of Leg Geometry on the Performance of Bi<sub>2</sub>Te<sub>3</sub> Thermoelectric Generators. *Gazi University Journal of Science* 37:1752–1768. <https://doi.org/10.35378/gujs.1420942>
- Hasan MK, Üstüner MA, Mamur H, Bhuiyan MRA (2024c) Enhancing Bi<sub>2</sub>Te<sub>2.70</sub>Se<sub>0.30</sub> Thermoelectric Module Performance through COMSOL Simulations. *Thermo* 4:185–201. <https://doi.org/10.3390/thermo4020011>
- Hashemi Fath A, Pouranfard A, Foroughizadeh P (2018) Development of an artificial neural network model for prediction of bubble point pressure of crude oils. *Petroleum* 4:281–291. <https://doi.org/10.1016/j.petlm.2018.03.009>
- Hofny MS, Ghazaly NM, Shmroukh AN, Abouelsoud M (2024) Evaluation of ethanol-gasoline blends in SI engines using experimental and ANN techniques. *Eng Res Express* 6:035517. <https://doi.org/10.1088/2631-8695/ad5f18>
- Ibrahim A (2022) Optimizing a spark-ignition engine fuelled with methane using a two-zone combustion model. *Energy Storage and Saving* 1:272–283. <https://doi.org/10.1016/j.enss.2022.09.002>
- Khedri B, Mostafaei M, Safieddin Ardebili SM (2019) A review on microwave-assisted biodiesel production. *Energy Sources, Part A: Recovery, Utilization, and Environmental Effects* 41:2377–2395. <https://doi.org/10.1080/15567036.2018.1563246>
- Kumar P, Dhingra AK, Chhabra D, Chhikara A (2023) Multi-objective parameter optimization for four-stroke single-cylinder diesel engine with soyabean oil blends using NSGA-II. *Eng Res Express* 5:045012. <https://doi.org/10.1088/2631-8695/acfb8>
- Kumar S (2021) Production and optimization from Karanja oil by adaptive neuro-fuzzy inference system and response surface methodology with modified domestic microwave. *Fuel* 296:120684. <https://doi.org/10.1016/j.fuel.2021.120684>
- Modi MA, Patel TM (2023) Experimental investigation of emission parameters of diesel engine fueled with various plastic pyrolysis oils. *International Journal of Engineering, Science and Technology* 15:1–10. <https://doi.org/10.4314/ijest.v15i3.1>

10.48047/jocaaa.2024.33.08.226

- Modi MA, Patel TM (2024a) Modeling of specific fuel consumption for compression ignition engines fueled with polymer-based fuel: a response surface methodology approach. *Eng Res Express* 6:035567. <https://doi.org/10.1088/2631-8695/ad78ab>
- Modi MA, Patel TM (2024b) Predictive modeling of specific fuel consumption in compression ignition engines using neural networks: a comparative analysis across diesel and polymer-based fuels. *Eng Res Express* 6:035519. <https://doi.org/10.1088/2631-8695/ad62b5>
- Mohan B, Yang W, Raman V, Sivasankaralingam V, Chou SK (2014) Optimization of biodiesel fueled engine to meet emission standards through varying nozzle opening pressure and static injection timing. *Applied Energy* 130:450–457. <https://doi.org/10.1016/j.apenergy.2014.02.033>
- Mwenge P, Rutto H (2025) Machine learning-based predictive modelling of biodiesel production from animal fats catalysed by a blast furnace slag geopolymer. *Results in Engineering* 25:104126. <https://doi.org/10.1016/j.rineng.2025.104126>
- Pradhan D, Singh RK, Bendu H, Mund R (2016) Pyrolysis of Mahua seed (*Madhuca indica*) – Production of biofuel and its characterization. *Energy Conversion and Management* 108:529–538. <https://doi.org/10.1016/j.enconman.2015.11.042>
- Raja K, Packiyam T, Saravanan A, Yaashikaa PR, Vickram AS (2025) Assessing the techno-economic and sustainable potential of chemical looping for bioenergy production from organic solid wastes. *Energy Storage and Saving* 4:14–26. <https://doi.org/10.1016/j.enss.2024.11.007>
- Shah MdS, Hasan MdK, Barman SC, Bhuiyan JA, Mamur H, Bhuiyan MRA (2025) Enhancing PV performance of Al/ZnO/CdS/GaAs/NiO/Au solar cells through diverse layer combinations by SCAPS-1D. *Next Research* 2:100143. <https://doi.org/10.1016/j.nexres.2025.100143>
- Sikder S, Hasan MdK, Mamur H, Bhuiyan MRA (2025) Optimizing layer configuration and material selection to enhance CIGS solar cell performance through computational simulation. *Hybrid Advances* 10:100460. <https://doi.org/10.1016/j.hybadv.2025.100460>
- Verma P, Sharma MP (2016) Review of process parameters for biodiesel production from different feedstocks. *Renewable and Sustainable Energy Reviews* 62:1063–1071. <https://doi.org/10.1016/j.rser.2016.04.054>
- Wiloso EI, Heijungs R, de Snoo GR (2012) LCA of second generation bioethanol: A review and some issues to be resolved for good LCA practice. *Renewable and Sustainable Energy Reviews* 16:5295–5308. <https://doi.org/10.1016/j.rser.2012.04.035>
- Youssef A, Ibrahim A (2024) NO<sub>x</sub> emissions reduction through applying the exhaust gas recirculation (EGR) technique for a diesel engine fueled with a diesel-biodiesel-diethyl ether blend. *Energy Storage and Saving* 3:318–326. <https://doi.org/10.1016/j.enss.2024.10.003>